to invite dissociation to $[SO_2]^-$. It may be, therefore, that the unusual situation occurs in *aqueous* media, where $[S_2O_4]^{2-}$ is the predominant species, and that H_2O and/or OH^- can somehow stabilize the dimeric S–S-bonded species. Anticipated studies of the temperature dependence of K_{eq} will result in enthalpy and entropy data, which should provide additional information about the solvation of the radical anion by organic solvents, another obvious possibility to explain the much increased dissociation in these media.

A form of dithionite which is soluble in nonaqueous media may be a useful reagent for many organic synthetic procedures that now involve $Na_2S_2O_4$. As we have shown, the use of solvents that contain limited amounts of (or no) H_2O will result in dramatically higher concentrations of $[SO_2]^-$, a situation that either could make a known "dithionite reduction" more facile or could result in the formation of new products. $[Et_4N]_2[S_2O_4]$ may also be an effective reductant for various transition-metal species, which are insoluble in water and therefore not susceptible to reduction by $Na_2S_2O_4$. Finally, the characterization of the dithionite/sulfur dioxide radical anion system may be relevant to the design and development of the lithium–sulfur dioxide battery,[31] the driving force for some[30] of the above work on the electroreduction of SO_2. In this context, additional knowledge of the nature of the products formed on reaction of SO_2 with mixtures of $[S_2O_4]^{2-}$ and $[SO_2]^-$, where both $[S_2O_4]^-$[25–30] and $[S_3O_6]^{2-}$[28] have been implicated, is particularly important.

Acknowledgment. We thank Drs. Gerald D. Watt and James L. Corbin for many helpful discussions. This work was supported by Grant 85-CRCR-1-1639 from the USDA/SEA Competitive Grants Research Office.

(31) Kilroy, W. P. In "28th Power Sources Symposium"; The Electrochemical Society: Princeton, NJ, 1978; p 198.

Contribution from the Department of Chemistry, The University of North Carolina, Chapel Hill, North Carolina 27514

Synthesis and Redox Properties of the Unsymmetrical, Oxo-Bridged Complex $[(bpy)_2(py)Ru^{III}ORu^{III}(H_2O)(bpy)_2]^{4+}$

Pascal Doppelt[1] and Thomas J. Meyer*

Received May 16, 1986

The μ-oxo ions $[(bpy)_2(L)Ru^{III}ORu^{III}(py)(bpy)_2]^{4+}$ (bpy = 2,2′-bipyridine, py = pyridine, L = py or H_2O) have been prepared and their redox properties in water and acetonitrile investigated by electrochemical techniques. The bis(pyridine) μ-oxo ion is unstable toward ligand loss in acetonitrile or water, giving initially the solvated ions $[(bpy)_2(S)Ru^{III}ORu^{III}(py)(bpy)_2]^{4+}$ (S = CH_3CN, H_2O). In water the mixed aqua pyridine ion undergoes successive 1-electron oxidations to give successively the Ru(IV)–Ru(III) and then the Ru(V)–Ru(III) ion $[(bpy)_2(O)Ru^{V}ORu^{III}(py)(bpy)_2]^{4+}$. Comparisons with related aqua/oxo monomeric couples suggest that the $[(bpy)_2(py)Ru^{III}–O–]^+$ group acts as an electron-rich "substituent" and is important in allowing the aqua site to reach Ru(V) within the oxidative limits of the solvent. The Ru(V)–Ru(III) form of the μ-oxo ion acts as an effective electrocatalyst for the oxidation of Cl^- to Cl_2 at pH <4 and of Cl^- to OCl^- at pH >11.8 where the oxidations are thermodynamically spontaneous. Water is slowly oxidized to O_2 in acidic solutions containing the mixed aqua pyridine μ-oxo ion and a large excess of Ce(IV).

Introduction

From the results of pH-dependent electrochemical studies, the μ-oxo ion $[(bpy)_2(OH_2)Ru^{III}ORu^{III}(OH_2)(bpy)_2]^{4+}$ (bpy is 2,2′-bipyridine) undergoes a sequence of electron–proton losses, ultimately to reach $[(bpy)_2(O)Ru^{V}ORu^{V}(O)(bpy)_2]^{4+}$. The Ru(V)–Ru(V) ion in turn oxidizes water to oxygen and provides a basis for the catalytic oxidation of water to oxygen via[2]

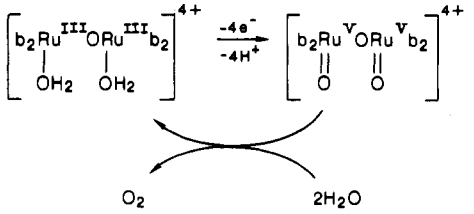

(b = bpy). The μ-oxo structure appears to play an important role in water oxidation in the following ways: (1) The $4e^-/4H^+$ requirement for water oxidation

$$2H_2O \rightarrow O_2 + 4e^- + 4H^+$$

is met by the sequential loss of electrons and protons in the oxidation of the III,III ion to the V,V ion. (2) If there is an O–O coupling requirement in the mechanism, it is met by the close proximity of the $Ru^V{=}O$ groups.

We report here the preparation of the unsymmetrical μ-oxo ion $[(bpy)_2(OH_2)Ru^{III}ORu^{III}(py)(bpy)_2]^{4+}$ and a comparison of its redox properties with those of the diaqua ion. With the comparison we hoped to explore the implied importance of having two reactive sites in close proximity for water oxidation[3] and in the aqua pyridine dimer to investigate the $Ru^{III}—OH_2 \rightarrow Ru^V{=}O$ redox characteristics of the individual sites. A second basis for our interest in the unsymmetrical μ-oxo ion was the possibility of having access to a $Ru^V{=}O$ site in a chemically linked structure like

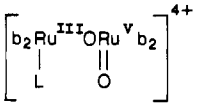

which opens the possibility of synthesizing a family of μ-oxo ions where systematic variations in L could lead to controlled perturbations at the $Ru^V{=}O$ site and possibly to the control of reactivity based on electronic, electrostatic, steric, or chiral effects.

Experimental Section

Materials. All reagents were reagent or ACS grade and used without purification. Elemental analyses were performed by Galbraith Laboratories, Knoxville, TN. The water used in analytical measurements was Aldrich HPLC grade.

Preparations. $[(bpy)_2(OH_2)RuORu(OH_2)(bpy)_2](ClO_4)_4 \cdot 2H_2O$ (**1**) was prepared as previously described.[2c]

(1) Institut Le Bel, Université Louis Pasteur, 67070 Strasbourg Cedex, France.

(2) (a) Gersten, S. W.; Samuels, G. J.; Meyer, T. J. *J. Am. Chem. Soc.* **1982**, *104*, 4029. (b) Ellis, C. D.; Gilbert, J. A.; Murphy, W. R., Jr.; Meyer, T. J. *J. Am. Chem. Soc.* **1983**, *105*, 4842. (c) Gilbert, J. A.; Eggleston, D. S.; Murphy, W. R.; Geselowitz, D. A.; Gersten, S. W.; Hodgson, D. J.; Meyer, T. J. *J. Am. Chem. Soc.* **1985**, *107*, 3855. (d) Honda, K., Frank, A. J. *J. Chem. Soc. Chem. Commun.* **1984**, 1635. (e) Collin, J. P.; Sauvage, J. P. *Inorg. Chem.* **1986**, *25*, 135.

(3) Geselowitz, D. A.; Kutner, W.; Meyer, T. J. *Inorg. Chem.* **1986**, *25*, 2015.

0020-1669/87/1326-2027$01.50/0

$[(bpy)_2(py)RuORu(py)(bpy)_2](ClO_4)_4 \cdot 4H_2O$. A 0.5-g sample of **1** was dissolved in 10 mL of pyridine. The solution was stirred for 1 h at room temperature and 20 min at 40 °C. When the solution was cooled to room temperature, a blue-green precipitate appeared, which was filtered off, washed with diethyl ether, and air dried. The compound was recrystallized by dissolving in 100 mL of distilled water and adding 2 g of $NaClO_4 \cdot H_2O$. After the mixture was cooled overnight, the resulting blue crystalline compound was filtered, washed with a 50%/50% ethanol/ether solution and finally with diethyl ether, and air dried. Yield: 75%. Anal. Calcd: C, 40.8; H, 3.4; N, 9.5. Found: C, 41.2; H, 3.6; N, 9.4.

$[(bpy)_2(OH_2)RuORu(py)(bpy)_2](ClO_4)_4$. Synthesis 1. A 0.1-g sample of $[(bpy)_2(py)RuORu(py)(bpy)_2](ClO_4)_4 \cdot 4H_2O$ was dissolved in 10 mL of an aqueous NaOH solution (0.1 M). The solution was gently heated (45–50 °C) for 15 min and then cooled to room temperature; 2 mL of a $LiClO_4$-saturated aqueous solution was added and then the solution cooled overnight. Blue crystals of the dimer were collected on a medium frit, washed with 1 mL of cold distilled water and then with a 50%/50% ethanol/ether solution, and air dried. Yield: 60%. Anal. Calcd: C, 39.2; H, 3.4; N, 9.1. Found: C, 40.2; H, 3.4; N, 9.2.

Synthesis 2. A 0.5-g sample of **1** was dissolved in 10 mL of pyridine. The solution was stirred for 1 h at 0 °C and then poured into 100 mL of diethyl ether. The blue gummy precipitate was crystallized in the same way as described for the bis(pyridine)(μ-oxo) ion. Yield: 60–70%. Anal. Calcd: C, 39.3; H, 3.4; N, 9.1. Found: C, 39.8; H, 3.7; N, 8.9.

Measurements. Cyclic voltammetric measurements were carried out by using a PAR Model 173 potentiostat/galvanostat or a PAR 264A polarographic analyzer. Coulometric measurements were made on a PAR Model 179 digital coulometer. Cyclic voltammetric measurements were made by using activated-glassy-carbon working electrodes[4] or an electrode fashioned from coarse (12 holes by linear in.) reticulated vitreous carbon (ERG Inc.) connected with a copper wire by using conductive carbon paint (SPI supplies). A platinum-wire auxiliary electrode and a saturated sodium chloride calomel (SSCE) reference electrode were also used in a three-compartment cell arrangement. The concentration of dimers used was approximately 0.5 mM. In aqueous solutions the pH was adjusted from 0 to 2 with trifluoromethanesulfonic acid, sodium trifluoromethanesulfonate being added to keep a minimum ionic strength of 0.1 M, and from 2 to 12 with 0.1 M phosphate buffers. Dilute NaOH solutions were used to achieve pH 12–13 with sodium trifluoromethanesulfonate added as electrolyte. All $E_{1/2}$ values reported were estimated for cyclic voltammetry as the average of the oxidative and reductive peak potentials, $(E_{p_a} + E_{p_c})/2$. UV–visible spectra were recorded on a Bausch & Lomb spectrophotometer using matched quartz 1-cm cells.

Results

Preparation and Solution Properties of the μ-Oxo Ions. We have developed two synthetic procedures for the preparation of the mixed μ-oxo aqua pyridine ion, the first based on aqua substitution in $[(bpy)_2(H_2O)Ru^{III}ORu^{III}(H_2O)(bpy)_2]^{4+}$ which for Cl^- is known to occur stepwise.[2b] In neat pyridine, disubstitution occurs at 40–50 °C

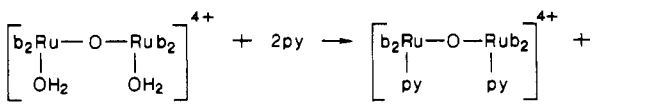

while at 0 °C substitution can be limited to a single site

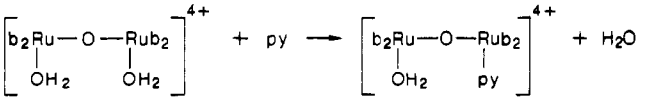

The second synthetic approach involves loss of pyridine from $[(bpy)_2(py)RuORu(py)(bpy)_2]^{4+}$

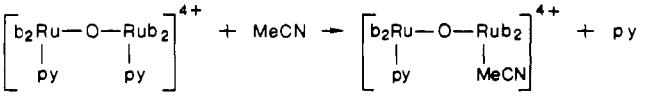

which in neat acetonitrile occurs with a half-time of ~9.5 h at 23 °C (Figure 1A) and is complicated by the slower loss of a second pyridyl group.

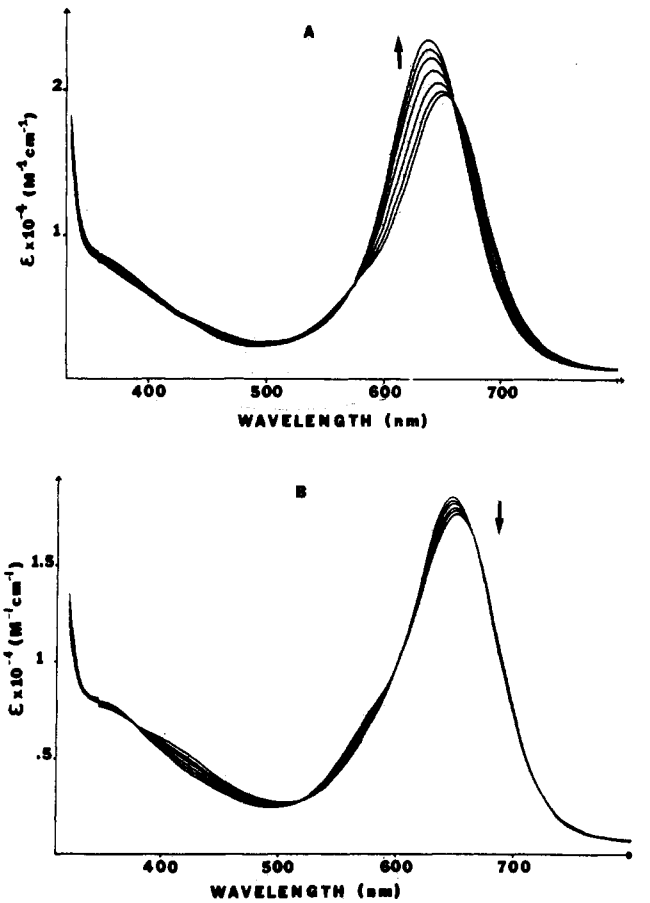

Figure 1. Spectral changes for $[(bpy)_2(py)RuORu(py)(bpy)_2]^{4+}$: (A) dissolved in neat acetonitrile at 1-h intervals except for the last spectrum, which was recorded 12 h after beginning the experiment. (B) dissolved in aqueous solution at pH 9 at 15-min intervals, the last spectrum was recorded 4 h after beginning the experiment.

In aqueous basic solution loss of the first pyridine group (Figure 1B)

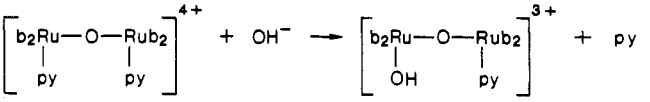

is pH dependent with reaction half-lives at pH 8.0, 9.0, and 10.0 of ~6, ~0.8, and ~0.35 h, respectively. The appearance of an apparent base-catalyzed pathway for ligand loss in the dimer is notable but we have not explored the point in detail.

Redox Properties. Electrochemical data for a series of μ-oxo ions in acetonitrile are given in Table I. Characteristically two reversible waves appear in the accessible potential region arising from 1-electron oxidation and 1-electron reduction of the μ-oxo III,III ions, e.g., for the bis(pyridine) ion

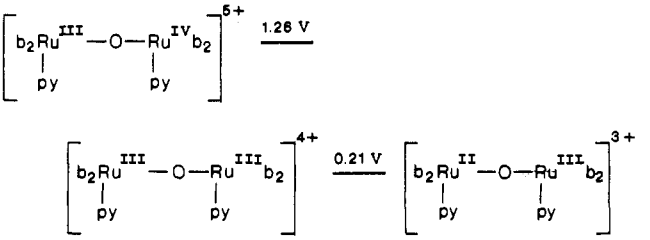

(vs. SSCE in CH_3CN). An additional, irreversible reduction is observed at more negative potentials, which leads to reductive decomposition of the μ-oxo bridge.[2c,5]

(4) (a) Diamantis, A. A.; Murphy, W. R.; Meyer, T. J. *Inorg. Chem.* **1984**, *23*, 3230. (b) Cabaniss, G. E.; Diamantis, A. A.; Murphy, W. R.; Linton, R. W.; Meyer, T. J. *J. Am. Chem. Soc.* **1985**, *107*, 1845–1853.

(5) Weaver, T. R.; Meyer, T. J.; Adeyemi, S. A.; Brown, G. M.; Eckberg, R. P.; Hatfield, W. E.; Johnson, E. C.; Murray, R. W.; Untereker, D. *J. Am. Chem. Soc.* **1975**, *97*, 3039.

Table I. Formal Reduction Potentials in 0.1 M $(NEt_4)(ClO_4)$–Acetonitrile vs. SSCE at 23 ± 2 °C (b = 2,2′-Bipyridine)[a]

dimer	$E°'$(IV,III/III,III), V	$E°'$(III,III/III,II), V	$E°'$(III,II/II,II), V
$[b_2Ru(Cl)-O-Ru(Cl)b_2]^{2+}$ [b]	0.68	−0.32	−1.0
$[b_2Ru(NO_2)-O-Ru(NO_2)b_2]^{2+}$ [b]	0.94	−0.15	−0.75
$[b_2Ru(NCMe)-O-Ru(NCMe)b_2]^{4+}$ [c]	1.16	0.04	
$[b_2Ru(py)-O-Ru(NCMe)b_2]^{4+}$	1.27	0.18	−0.69
$[b_2Ru(py)-O-Ru(py)b_2]^{4+}$	1.26	0.21	−0.71

[a] From $E_{1/2}$ values assuming that diffusion coefficient corrections are negligible. [b] Reference 5. [c] By solvolysis of the bis(pyridine) dimer in CH_3CN after 24 h at room temperature.

Oxidation state labels like IV,III are used here for convenience. Strong electronic coupling exists between the μ-oxo-bridged sites leading, for example, to possible delocalization in the mixed-valence ion where a more appropriate oxidation-state description may be III.5,III.5.

Compared to the analogous (μ-oxo)dichloro ion,[5] potentials for the bis(acetonitrile), bis(pyridine), and the solvento(pyridine) ions are shifted oxidatively (Table I). The IV,III ion, $[(bpy)_2(py)Ru^{III}ORu^{IV}(py)(bpy)_2]^{5+}$, can be reached by Ce(IV) oxidation in acidic solution and isolated as its ClO_4^- salt, but the salt is unstable toward reduction in the solid state especially in the presence of organic vapors. Coulometric reduction of the III,III bis(pyridine) ion in acetonitrile past the III,II → II,II wave at −0.71 V occurs with n = 1.9, resulting in quantitative reductive decomposition of the dimer to give $[(bpy)_2(py)Ru(CH_3CN)]^{2+}$,[6] as shown by absorption spectral measurements. The wave at −0.71 V is completely irreversible at a scan rate of 50 mv/s.

In the cyclic voltammograms of $[(bpy)_2(H_2O)RuORu(py)(bpy)_2]^{4+}$ at pH 5 and 11 in Figure 2, waves for two one-electron oxidations and a two-electron reduction appear. Coulometric reduction at E_{app} = −0.3 V (n = 2.0 ± 0.1) gives $[(bpy)_2(py)Ru(OH_2)]^{2+}$ and $[(bpy)_2Ru(OH_2)_2]^{2+}$ [8a] via the net reaction

$$3H^+ + [b_2Ru(OH)-O-Rub_2(py)]^{3+} + 2e^- + H_2O \rightarrow [b_2(py)Ru(OH_2)]^{2+} + [b_2Ru(OH_2)_2]^{2+}$$

Below pH 6, the reductive wave is chemically irreversible on the cyclic voltammetry time scale (50 mv/s) as found earlier for related (μ-oxo)ruthenium[2c] and -osmium ions,[9] suggesting that a general acid-catalyzed pathway exists for decomposition of the reduced μ-oxo ions.

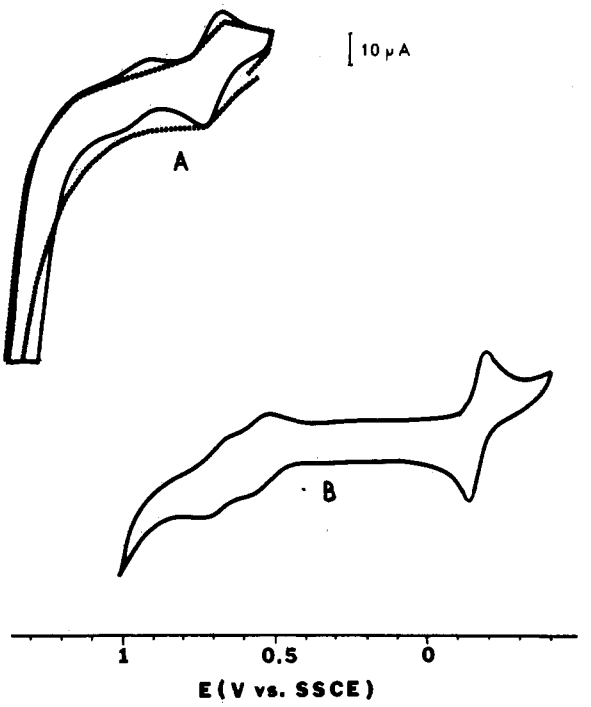

Figure 2. Cyclic voltammograms of $[(bpy)_2(H_2O)Ru^{III}ORu^{III}(py)(bpy)_2]^{4+}$: (A) pH 5; (B) pH 11.3. For voltammogram A the importance of electrode effects is also illustrated. The electrode used to acquire the dashed-line voltammogram was an activated-glassy-carbon electrode,[4] the full-line voltammogram was obtained by using a porous carbon electrode (see Experimental Section).

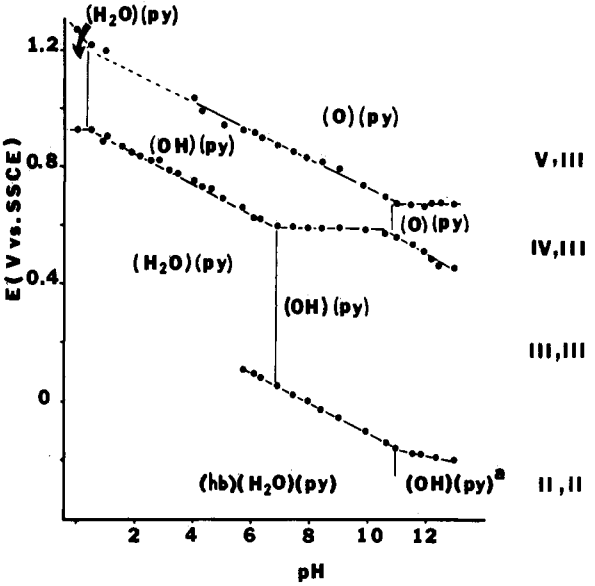

Figure 3. $E_{1/2}$ vs. pH or Pourbaix diagram derived from electrochemical measurements on the complex $[(bpy)_2(H_2O)Ru^{III}ORu^{III}(py)(bpy)_2]^{4+}$. The potential–pH regions where the various oxidation states of the dimer are the dominant forms are indicated by the designations III,III etc. The dominant proton compositions for the various oxidation states are indicated using abbreviations such as III,III–(OH)(py) for $[(bpy)_2(OH)Ru^{III}ORu^{III}(py)(bpy)_2]^{3+}$. pK_a values are shown by the vertical lines in the various E–pH regions. The abbreviation (hb) in $(hb)(H_2O)(py)$ refers to protonation at the oxo bridge to give $[(bpy)_2(H_2O)Ru^{II}(OH)Ru^{II}(py)(bpy)_2]^{3+}$. The reduced form of the complex could be either $[(bpy)_2(H_2O)Ru^{II}ORu^{II}(py)(bpy)_2]^{2+}$ or $[(bpy)_2(OH)Ru^{II}(OH)Ru^{II}(py)(bpy)_2]^{2+}$ (see text).

(6) Moyer, B. A.; Keith Sipe, B.; Meyer, T. J. *Inorg. Chem.* **1981**, *20*, 1475.
(7) Moyer, B. A.; Meyer, T. J. *Inorg. Chem.* **1981**, *20*, 436.
(8) (a) Takeuchi, K. J.; Samuels, G. J.; Gersten, G. J.; Gersten, S. W.; Gilbert, J. A.; Meyer, T. J. *Inorg. Chem.* **1983**, *22*, 1409. (b) Che, C.-M.; Wong, K.-Y.; Mak, T. C. U. *J. Chem. Soc. Chem. Commun.* **1985**, 546. (c) Yukawa, Y.; Aoyagi, K.; Kurihara, M.; Shirai, K.; Shimizu, K.; Mukradida, M.; Takeuchi, T.; Kakihana, H. *Chem. Lett.* **1985**, 283.
(9) Gilbert, J. A.; Geselowitz, D. A.; Meyer, T. J. *J. Am. Chem. Soc.* **1986**, *108*, 1493.
(10) (a) Roecker, L.; Kutner, W.; Gilbert, J. A.; Simmons, M.; Murray, R. W.; Meyer, T. J. *Inorg. Chem.* **1985**, *24*, 3784. (b) Ghosh, P. K.; Brunschwig, B. S.; Chou, M.; Creutz, C.; Sutin, N. *J. Am. Chem. Soc.* **1984**, *106*, 4772.
(11) Takeuchi, K. J.; Thompson, M. S.; Pipes, D. W.; Meyer, T. J. *Inorg. Chem.* **1986**, *23*, 1845.

Table II. Formal Reduction Potentials (V vs. SSCE at 23 °C)[a] in 1 M Triflic Acid

dimer	$E°'$(Couple), V IV,III/III,III	V,III/IV,III
$[(bpy)_2(OH_2)Ru-O-Ru(bpy)_2(OH_2)]^{4+}$[b]	0.81	>1.3
$[(bpy)_2(OH_2)Ru-O-Ru(bpy)_2(py)]^{4+}$	0.94	1.36
$[(bpy)_2(py)Ru-O-Ru(bpy)_2(py)]^{4+}$	1.12	

[a] Estimated from $E_{1/2}$ values. [b] Reference 2c.

The dimer waves are pH dependent, and additional complications arise because of slow, electrode-dependent heterogeneous charge transfer, especially for the second oxidation as the pH is decreased. Similar observations have been made for related couples and attributed to slow electrode kinetics arising from the necessity of proton gains or losses in the net electrode reactions.[4]

The pH dependences of the various couples as derived from pH-dependent cyclic measurements are illustrated in the Pourbaix diagram in Figure 3. In Figure 3 abbreviations like (IV,-III)-(OH)(py) for the ion $[(bpy)_2(OH)Ru^{IV}ORu^{III}(py)(bpy)_2]^{4+}$ are used to identify oxidation state and proton composition, pK_a values derived from the breaks in the $E_{1/2}$–pH plots are shown as vertical lines, and the slopes of the lines, $-m/n(0.059)$, follow from the Nernst equation, where m is the number of protons gained in the lower oxidation state and n is the number of electrons.

From its $E_{1/2}$–pH dependence above pH 11 (28 mV/pH unit), the III,III/II,II couple can be written as

$$[b_2Ru^{III}-O-Ru^{III}b_2(OH)(py)]^{3+} + H_2O + 2e^- \rightarrow [b_2Ru^{II}-O-Ru^{II}b_2(OH_2)(py)]^{2+} + OH^-$$

However, the proton-dependent $E_{1/2}$ studies only give proton content and not structural information, and as noted below, it is conceivable that in the II,II form of the couple the proton is actually added to the oxo bridge giving

$$[b_2Ru^{II}-O(H)-Ru^{II}b_2(OH)(py)]^{2+}$$

At pH <11.0 the $2e^-/2H^+$ nature of the couple (59 mV/pH unit) essentially demands that protonation occur at both the Ru^{II}–OH and μ-oxo bridge sites

$$[b_2Ru^{III}-O-Ru^{III}b_2(OH)(py)]^{3+} + 2H_2O + 2e^- \rightarrow [b_2Ru^{II}-O(H)-Ru^{II}b_2(OH_2)(py_2)]^{3+} + 2OH^-$$

There is also a possible ambiguity with regard to the V,III/IV,III couple in strongly acidic solution. For the bis(pyridine) dimer, the pH-independent IV,III/III,III couple occurs at $E_{1/2}$ = 1.12 V (Table II). If the $[(bpy)_2(py)Ru^{IV/III}-]$ couple in the aqua pyridine dimer were also at 1.12 V, the $[(bpy)_2(py)Ru^{IV/III}-]$ and $[-Ru^{V}(O)(bpy)_2]/[-Ru^{IV}(OH)(bpy)_2]$ couples would overlap in potential at pH ~2. At pH <2 a pH-independent wave for the Ru–py-based IV/III couple, as well as a pH-dependent wave for the Ru=O/Ru—OH-based V/IV couple, should appear. In fact, the pH dependence data are consistent with a (V,III/IV,III) couple, and the Ru–py-based IV/III couple must occur at $E_{1/2}$ > 1.26 V. The increase in potential for the Ru–py couple compared to its value in the py–py ion is probably attributable to a greater electronic deficiency arising from electronic coupling with the Ru^{V}=O or Ru^{IV}—OH sites in $[(bpy)_2(OH)Ru^{IV}ORu^{III}(py)(bpy)_2]^{4+}$ or $[(bpy)_2(O)Ru^{V}ORu^{III}(py)(bpy)_2]^{4+}$. Potentials for the diaqua, aqua pyridine, and bis(pyridine) dimers are compared in Table II.

Table III. Absorption Spectral Properties of the Intense Low-Energy Absorption Bands for the Dimers (b = 2,2′-Bipyridine)

dimer	medium	λ_{max}, nm (log ϵ)
$[b_2Ru^{III}OHRu^{III}b_2(py)(py)]^{4+}$	MeCN	640 (4.37)
	H_2O (pH 1)	640 (4.32)
$[b_2Ru^{III}OHRu^{IV}b_2(py)(py)]^{5+}$[a]	H_2O (pH 1)	450 (4.31)
$[b_2Ru^{III}OHRu^{III}b_2(py)(NCMe)]^{4+}$	MeCN	626 (4.44)
$[b_2Ru^{III}OHRu^{III}b_2(OH_2)(py)]^{4+}$	pH 1	636 (4.28)
$[b_2Ru^{III}OHRu^{III}b_2(OH)(py)]^{3+}$	pH 12.1	646 (4.21)
$[b_2Ru^{IV}OHRu^{III}b_2(OH_2)(py)]^{5+}$[a]	pH −0.2	446 (4.20)
$[b_2Ru^{IV}OHRu^{III}b_2(OH)(py)]^{4+}$[a]	pH 1	506 (4.23)

[a] By 1-equiv oxidation of the III,III dimer by Ce(IV).

Table IV. Acid Dissociation Constants at 23 °C, μ = 0.1 M[a] (b = 2,2′-Bipyridine)

monomer or dimer	pK_{a1}	pK_{a2}
$[b_2(H_2O)Ru^{III}ORu^{III}(H_2O)b_2]^{4+}$[b]	5.9	8.3
$[b_2(H_2O)Ru^{IV}ORu^{III}(H_2O)b_2]^{5+}$[b]	0.4	3.3
$[b_2(py)Ru^{II}(H_2O)]^{2+}$[c]	10.3, 10.8[b]	
$[b_2(py)Ru^{III}(H_2O)]^{3+}$[c]	0.85	>13
$[b_2(H_2O)Ru^{III}ORu^{III}(py)b_2]^{3+}$	6.8[d]	
$[b_2(H_2O)Ru^{IV}ORu^{III}(py)b_2]^{4+}$	0.3[e]	10.9[d]

[a] $Na^+CF_3SO_3^-$. [b] Reference 2c. [c] μ = 1.0 M.[11] [d] From the Pourbaix diagram in Figure 4. [e] By spectrophotometric titration; no correction for ionic strength ±0.2.

Spectra and pK_a Values. Absorption spectra for the III,III and IV,III aqua pyridine μ-oxo ions in acidic and basic solutions are shown in Figure 4. We were unable to obtain the spectrum of the doubly deprotonated IV,III ion, $[(bpy)_2(O)Ru^{IV}ORu^{III}(py)(bpy)_2]^{5+}$, because at the high pH values needed to remove the second proton from Ru(IV) (>10.9, Figure 4), net intramolecular oxidation of bpy is too rapid.

Spectral data for the low-energy, intense visible bands for the various μ-oxo ions are summarized in Table III, and in Table IV are gathered pK_a values for the unsymmetrical ion and, for purposes of comparison, pK_a values for related complexes. For the aqua pyridine ion pK_a values were derived from the breaks in the $E_{1/2}$ vs. pH plots in Figure 3 except for pK_{a1} for $[(bpy)_2(H_2O)Ru^{IV}ORu^{III}(py)(bpy)_2]^{5+}$, which was obtained by a spectrophotometric titration in triflic acid over the range $[H^+]$ = 2–0.1 M using ϵ values of 15 900 (λ = 447 nm) and 5980 M^{-1} cm^{-1} (λ

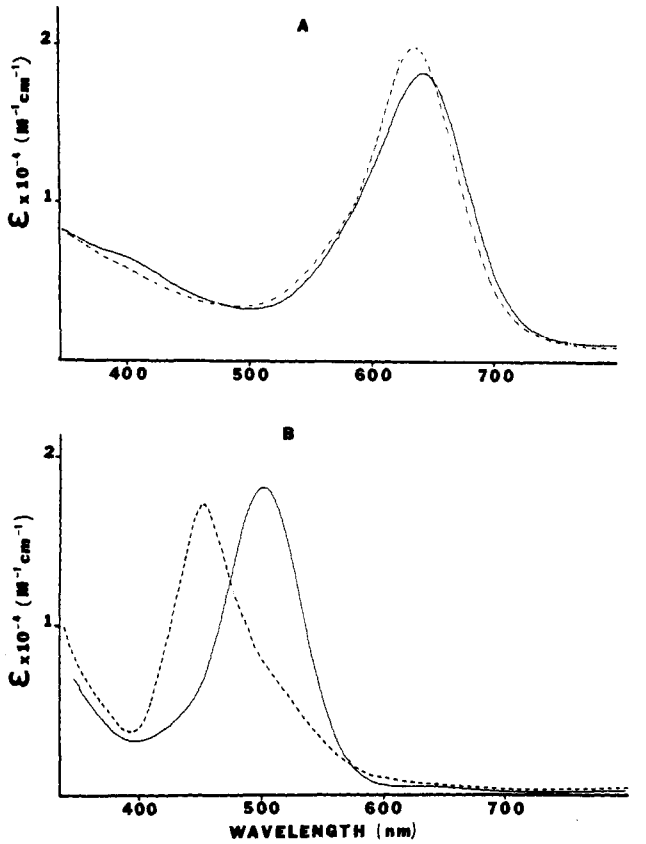

Figure 4. Visible spectra of aqueous solutions: (A) $[(bpy)_2(OH)Ru^{III}ORu^{III}(py)(bpy)_2]^{3+}$ at pH 12.2 (dashed line) and $[(bpy)_2(H_2O)Ru^{III}ORu^{III}(py)(bpy)_2]^{4+}$ at pH 1. (B) $[(bpy)_2(OH)Ru^{IV}ORu^{III}(py)(bpy)_2]^{4+}$ at pH 1 (full line) and $[(bpy)_2(H_2O)Ru^{IV}ORu^{III}(py)(bpy)_2]^{5+}$ at pH −0.1 (dashed line).

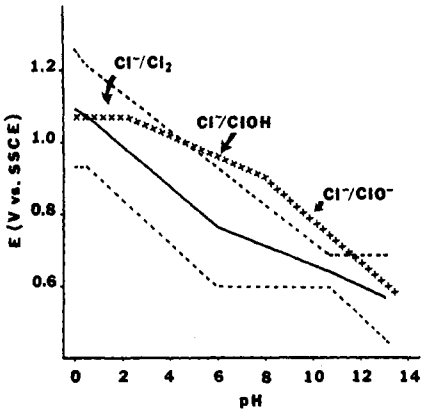

Figure 5. pH dependences of the couples interrelating $Cl^-/Cl_2/OCl^-/HOCl$ (×) and the V,III/IV,III and IV,III/III,III couples of $[(bpy)_2(H_2O)Ru^{III}ORu^{III}(py)(bpy)_2]^{4+}$ (dashed lines). The solid line shows the pH dependence of the 2-electron V,III/III,III couple calculated from the two 1-electron couples.

= 507 nm) for $[(bpy)_2(H_2O)Ru^{IV}ORu^{III}(py)(bpy)_2]^{5+}$ and $\epsilon \approx$ 17 000 (λ = 507 nm) and 4300 (λ = 447 nm) M^{-1} cm^{-1} for $[(bpy)_2(OH)Ru^{IV}ORu^{III}(py)(bpy)_2]^{4+}$.

Electrocatalytic Oxidation of Cl^- to Cl_2. In Figure 5 are illustrated the pH dependences of the couples that interrelate $Cl^-/Cl_2/OCl^-/HOCl$, the pH dependences of the μ-oxo IV,III/III,III and V,III/IV,III couples (dashed line), and the pH dependence of the 2-electron V,III/III,III couple calculated from the two 1-electron couples (solid line). From the diagram the following points can be made: (1) In acidic solution the V,III/IV,III couple is thermodynamically capable of Cl^- oxidation via the net reactions

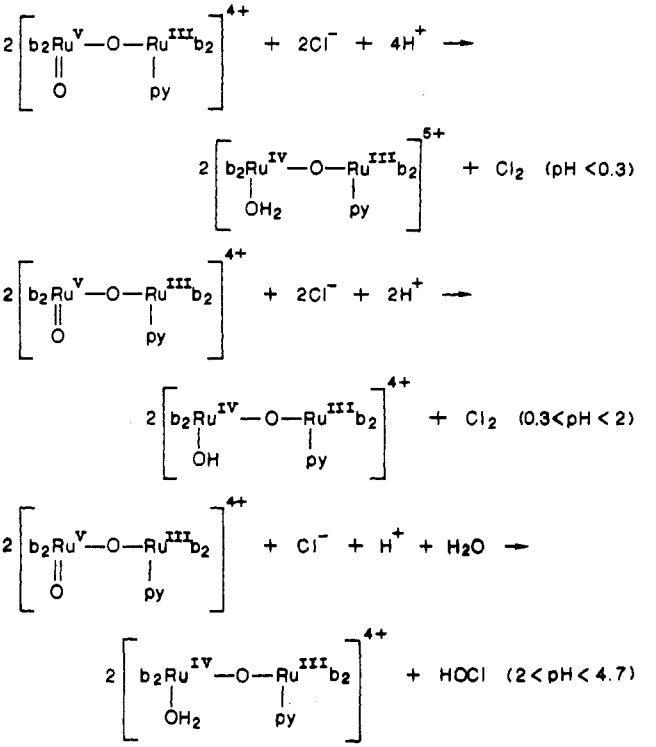

(2) As the pH is raised, the difference in H^+ (or OH^-) dependences between the dimer and Cl-based couples reverses the sense of the net chemistry

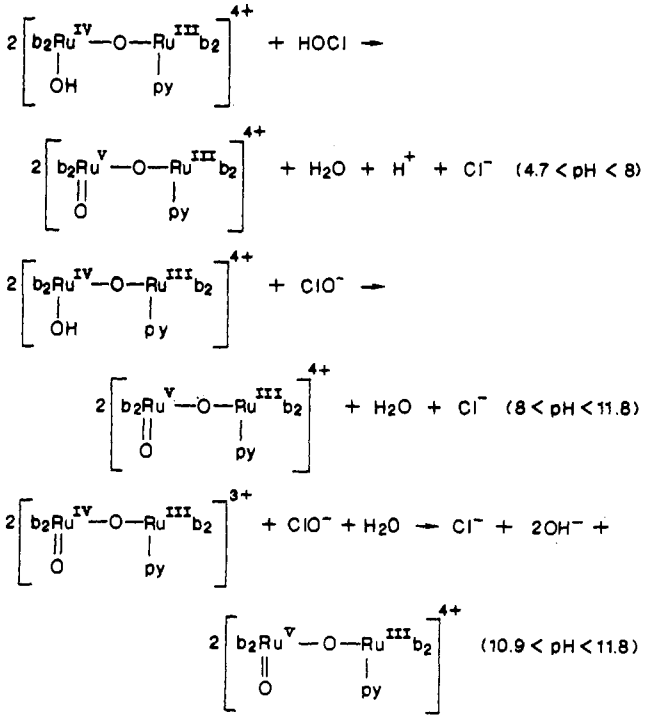

(3) At pH 10.9, the V,III/IV,III couple becomes independent of pH, and by pH 11.8, the net chemistry reverses again with the net reaction becoming

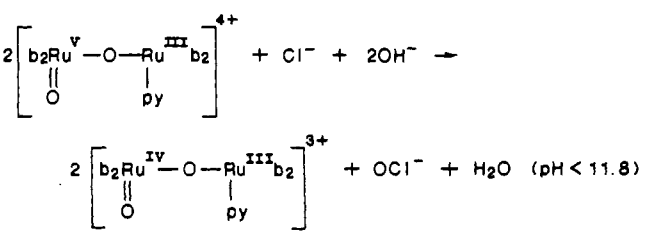

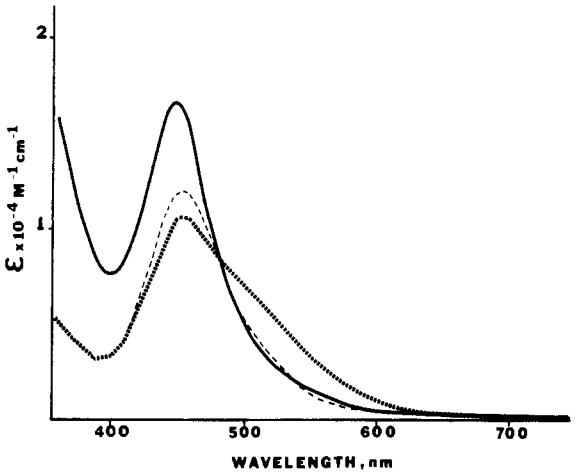

Figure 6. Visible spectra in 4 M triflic acid of $[(bpy)_2(H_2O)Ru^{IV}O\text{-}Ru^{III}(py)(bpy)_2]^{5+}$ (full line) and the same complex after the addition of 5 equiv of Ce(IV) after 1 h (small squares) and after 5 h (dashed line).

Cyclic voltammograms at pH 0, 8.2, and 12.2 verify the thermodynamic predictions and show that the net reactions written above are facile as found earlier for the V,IV form of the diaqua dimer.[2b,12] With added Cl^- (>1 mM) at pH 0 and 12.2 a significant catalytic current is observed at the onset of the Ru(IV) → Ru(V) wave as observed earlier for the aqua dimer while there is no sign of electrocatalytic oxidation of Cl^- in the range $4.7 < pH < 11.8$.

Oxidation of H_2O to O_2. In Figure 6 are shown spectral traces obtained after the addition of an excess of Ce(IV) to the IV,III dimer in 4 M triflic acid. Under these conditions the IV,III → V,III oxidation by Ce(IV) occurs with $\Delta G \sim 0$ since $E^{\circ\prime}$ (Ce(IV/III)) = 1.7 V (vs. NHE) in 1 M $HClO_4$ and $E^{\circ\prime}$ = 1.6 V (vs. NHE) for the V,III/IV,III couple at pH 0. In fact, in 4 M triflic acid the potential for the dimer couple is even higher given its squared dependence on pH (Figure 3) and oxidation by Ce(IV) appears to be thermodynamically nonspontaneous. From the spectral changes observed after the addition of excess (×5) Ce(IV) the following points can be made: (1) An initial decrease in absorbance occurs at 456 nm over a period of ~1 h for $[(bpy)_2(H_2O)Ru^{IV}ORu^{III}(py)(bpy)_2]^{5+}$ with a new feature appearing at $\lambda_{max} \sim 520$ nm. A reasonable interpretation is that the new band is associated with $[(bpy)_2(O)Ru^{V}ORu^{III}(py)(bpy)_2]^{4+}$ and the spectral evidence for the existence of both the IV,III and V,III dimers suggests that under these conditions the system is at or near equilibrium with the Ce(IV)/Ce(III) couple

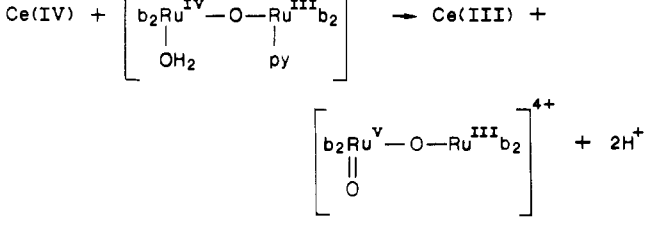

(2) On a longer time scale (hours) the band at ~520 nm decreases accompanied by the appearance of O_2 (see below). There is no significant decomposition of the dimer under these conditions. Addition of ascorbic acid as a reducing agent after 6 h gave back >80% of the III,III form of the dimer as shown by the intensity of the III,III band at 636 nm.

In the presence of a 50–100-fold excess of Ce(IV), the Ce(IV) is slowly ($t_{1/2} \sim 19$ h) reduced to Ce(III) as shown by the decrease in the Ce(IV) absorption at 303 nm. O_2 is produced under these conditions as shown by GC. With volume changes observed in a gastight apparatus, (1) the volume change of 0.3 mL (50 mg of added $Ce(NO_3)_6(NH_4)_2$) after 48 h was 60% of that expected for the amount of Ce(IV) added if O_2 were the product, and (2) ~100% of the expected volume change was observed after a week in agreement with the stoichiometry

$$4Ce(IV) + 2H_2O \rightarrow 4Ce(III) + O_2 + 4H^+$$

The evolution of O_2, and loss of Ce(IV), becomes even slower after an initial ~20-h period apparently because of chemical changes in the dimer. After extended periods, changes in λ_{max} and loss of catalytic activity by the dimer may be attributable to oxidatively induced anation to give $[(bpy)_2(CF_3SO_3)Ru^{IV}O\text{-}Ru^{III}(py)(bpy)_2]^{4+}$, which undergoes slow solvolysis to return to the aqua dimer and reenter the catalytic cycle.

Discussion

It has been shown here that the diaqua ion $[(bpy)_2(H_2O)Ru^{III}ORu^{III}(H_2O)(bpy)_2]^{4+}$ is a useful synthetic intermediate. This is an important observation since it opens the possibility of preparing a series of μ-oxo, mixed-ligand systems where the added group L can be used to control the redox properties and possibly the reactivity at the adjacent aqua site by electronic, steric, or electrostatic effects. It also opens the possibility of substrate binding at a site in close proximity to the reactive $Ru^V{=}O$ group.

Molecular models show that disubstitution by bulky ligands like pyridine results in considerable steric crowding at the μ-oxo bridge, which, in turn, may account for the fairly rapid base-catalyzed loss of pyridine in water. In solutions containing the monomer $[(bpy)_2(py)Ru^{III}(OH)]^{2+}$ we can find no evidence for the establishment of the equilibrium

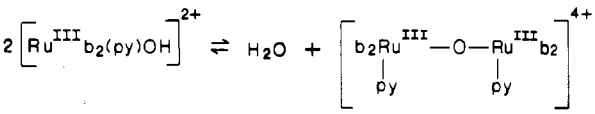

Redox Properties. Compositionally, the mixed μ-oxo pyridyl aqua ion is both a chemically modified form of the diaqua water oxidation catalyst and, when oxidized, a member of the class of monomeric polypyridyl Ru=O complexes like $[(bpy)_2(L)Ru{=}O]^{2+}$, in this case where the substituent L is $[(bpy)_2(py)Ru^{III}O]^+$. Comparisons with the monomer $[(bpy)_2(py)Ru^{IV}{=}O]^{2+}$[7] show that the $[(bpy)_2(py)Ru^{III}\text{–}O\text{–}]^+$ "substituent" is more electron rich and a net electron donor compared to pyridine. The evidence for this conclusion is the following: (1) $pK_{a1} = 6.8$ for $[(bpy)_2(H_2O)Ru^{III}ORu^{III}(py)(bpy)_2]^{4+}$ and 2.0 for $[(bpy)_2(py)Ru^{III}(H_2O)]^{3+}$. (2) Although there is no evidence for protonation of the oxo ligand in $[(bpy)_2(py)Ru^{IV}{=}O]^{2+}$ even in strongly acidic solution, the oxo group in $[(bpy)_2(O)Ru^{IV}ORu^{III}(py)(bpy)_2]^{3+}$ is singly protonated below pH 10.9 and doubly protonated past pH 0.3. (3) Oxidation state Ru(V) appears in the dimer while Ru(V) is not an accessible oxidation state in the monomer to the solvent limit of 1.6 V. It is interesting to note that for the related Os monomer $[(trpy)(bpy)Os(H_2O)]^{2+}$ (trpy = 2,2′,2″-terpyridine) a $[(trpy)(bpy)Os(O)]^{3+/2+}$ Os(V/IV) couple is observed at 1.05 V.[11]

In an oxidative sense the electron-rich $[(bpy)_2(py)Ru^{III}\text{–}O]^+$ substituent has the effect of greatly decreasing the potential of the Ru(IV/III) couple in the μ-oxo ion. For the couples $[(bpy)_2(L)Ru^{IV}(O)]^{2+}/[(bpy)_2(L)Ru^{III}(OH)]^{2+}$ at pH 11, $E_{1/2}$ values are 0.60 V vs. SSCE (L = $[(bpy)_2(py)Ru^{III}\text{–}O]^+$) and 0.36 V (L = py).

A second difference between the monomeric and μ-oxo-based couples occurs in basic solution and arises from the greater acidities of the Ru(III) and Ru(IV) sites in the μ-oxo ion compared to the Ru(II) and Ru(III) sites in the monomer (Table IV). For $[(bpy)_2(py)Ru^{II}(H_2O)]^{2+}$ $pK_{a1} = 10.3$, and above pH 10.3 the Ru(III/II) couple $[(bpy)_2(py)Ru(OH)]^{2+/+}$ becomes independent of pH. Past pH ~12, Ru(III) is unstable with respect to disproportionation into Ru(II) and Ru(IV) via

$$2[b_2(py)Ru^{III}\text{—}OH]^{2+} + OH^- \rightarrow [b_2(py)Ru^{II}\text{—}OH]^+ + [b_2(py)Ru^{IV}{=}O]^{2+} + H_2O$$

By contrast, in the μ-oxo ions a second proton is lost from Ru(IV)

(12) (a) Vining, W. J.; Meyer, T. J. *J. Electroanal. Chem. Interfacial Electrochem.* **1985**, *195*, 183–187. (b) Vining, W. J.; Meyer, T. J. *Inorg. Chem.* **1986**, *25*, 2023.

at pH 10.9, the V,III/IV,III couple *diverges* from the IV,III/III,III couple, and Ru(IV) is stable with respect to disproportionation over the entire pH range (Figure 3).

Because of the net electron-donating character of $[(bpy)_2(py)Ru^{III}–O–]^+$, the potentials of the Ru(V/IV) and Ru(IV/III) couples in the μ-oxo ion are sufficiently low that they have much in common with the Ru(IV/III) and Ru(III/II) couples of the monomer. In acidic solution, the μ-oxo-based Ru(IV/III) couple and monomer-based Ru(III/II) couple are thermodynamically nearly equivalent as 1-electron oxidants. Potentials for the $[(bpy)_2(L)Ru(OH)]^{2+}/[(bpy)_2(L)Ru(OH_2)]^{2+}$ couples at pH 2 are 0.83 V (L = $[(bpy)_2(py)Ru^{III}–O]^+$) for the Ru(IV/III) couple in the μ-oxo ion and 0.79 V (L = py) for the monomeric Ru(III/II) couple. However, the Ru(V/IV) couple in the μ-oxo ion ($E_{1/2}$ = 1.12 at pH 2) is considerably more strongly oxidizing than the Ru(IV/III) monomeric couple ($E_{1/2}$ = 0.88 at pH 2), which, if nothing else, is important in creating a more strongly oxidizing 2-electron Ru–oxo site in the dimer.

Revealing comparisons can also be made between the diaqua and aqua pyridine μ-oxo ions. At pH <0.3 the Ru(IV/III) couples $[(bpy)_2(H_2O)Ru^{IV/III}ORu^{III}(L)(bpy)_2]^{5+/4+}$ (L = py, H_2O) are pH independent and the slightly decreased potential for the diaqua μ-oxo ion (130 mV, Table II) suggests that as a substituent $[(bpy)_2(H_2O)Ru^{III}–O–]^+$ is only a slightly better election donor than is $[(bpy)_2(py)Ru^{III}–O–]^+$. The similarities extend to pK_a values where pK_{a1} values for the Ru(IV) sites in the two μ-oxo ions are ~0.3 for the mixed μ-oxo ion and ~0.4 for the diaqua ion and, for the Ru(III) sites, ~6.8 for the μ-oxo ion and ~5.9 for the diaqua ions. By contrast the $[(bpy)_2(OH)Ru^{III}–O–]$ group is considerably more electron donating than is $[(bpy)_2(py)Ru^{III}–O–]^+$. Potentials for the pH-independent IV,III/III,III couples $[(bpy)_2(OH)Ru^{IV/III}ORu^{III}(OH)(bpy)_2]^{3+/2+}$ and $[(bpy)_2(OH)Ru^{IV/III}ORu^{III}(py)(bpy)_2]^{4+/3+}$ are 0.22 and 0.60 V, respectively.

Reductively, both μ-oxo III,III ions undergo 2-electron reductions via III,III/II,II couples without evidence for intermediate III,II mixed-valence ions. Below pH 10.9 the $2e^-/2H^+$ nature of the mixed-ligand couple suggests protonation at the bridge

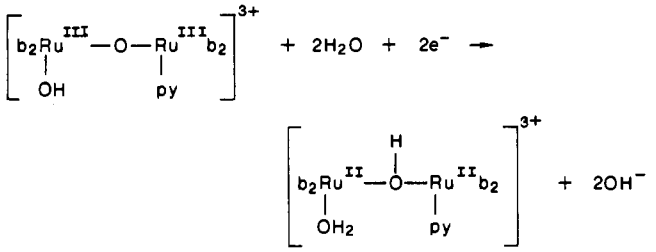

Above pH 10.9 the site of protonation is equivocal and could occur either at the μ-oxo or terminal hydroxo groups

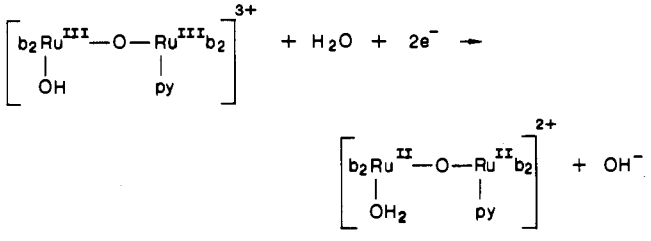

or

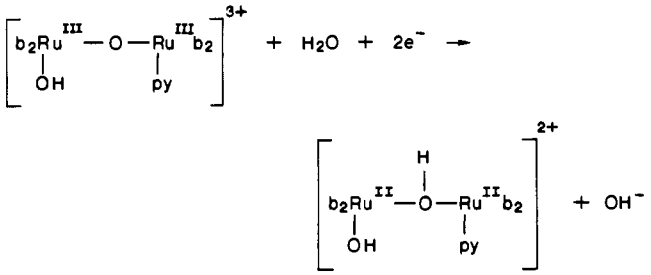

The nonappearance of a mixed-valence III,II ion in water is especially striking given the appearance of III,III/II,III and III,II/II,II couples separated by 0.92 V in acetonitrile (Table I). From the redox potential data, in water the diaqua and mixed-ligand III,II μ-oxo ions are unstable with respect to disproportionation over the whole pH range from 2 to 14 (Figure 3) while the bis(pyridine) dimer in acetonitrile is *stable* with respect to disproportionation by 0.92 V. The key to the instability of the mixed-valence ions in water may be stabilization of the II,II form by protonation at the oxo bridge. Qualitative molecular orbital based arguments suggest that addition of electrons to the μ-oxo III,III ion occurs at orbitals that are largely π-antibonding in character with regard to the Ru–O–Ru bridge.[5] Protonation could have a significant electronic stabilization effect in the electron-rich, fully reduced II,II ion. It is notable in this regard that reduction to the II,II ions in water is followed by relatively slow bridge cleavage, for example, to give $[(bpy)_2Ru^{II}(H_2O)_2]^{2+}$ for the diaqua dimer. The second reduction of $[(bpy)_2(py)RuORu(py)(bpy)_2]^{4+}$ or of $[(bpy)_2ClRuORuCl(bpy)_2]^{2+}$ in polar organic solvents in the absence of an added proton source leads to rapid cleavage.

Oxidation of Cl^- to Cl_2 and of H_2O to O_2. Even though we have been unable to obtain quantitative kinetics data on the oxidation of Cl^- to Cl_2 or of H_2O to O_2, the appearance of such reactivity for the mixed μ-oxo ion is notable. When oxidized, both the diaqua and aqua pyridyl μ-oxo ions become facile oxidants for the oxidation of Cl^- to Cl_2/HOCl/OCl^-. Mechanistically, even though the one-electron V,III/IV,III couple for the aqua pyridyl ion is involved in the net sense, the reaction may take advantage of the 2-electron capability of the V,III/III,III couple in an initial step

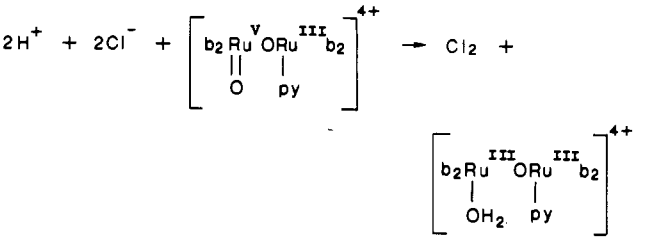

ΔG = +0.25 V (pH 0)

which, even though nonspontaneous, would avoid 1-electron intermediates and be followed by rapid comproportionation

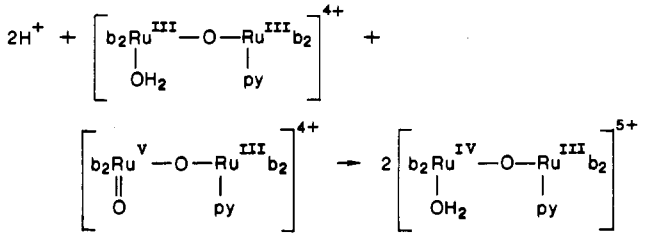

Although we do not yet have direct evidence, the key to the rapid rates may lie in Cl^- attack at the terminal oxo group

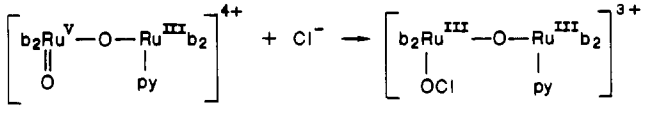

followed by loss of HOCl or OCl^- by solvolysis or of Cl_2 by Cl^- attack on bound OCl^- or bound HOCl.

The oxidation of water by the oxidized form of the mixed-ligand ion may be intrinsic. However, the possibility also exists that water oxidation occurs via partial loss of pyridine and formation of small amounts of the diaqua dimer, which is the actual catalyst for the reaction. In either case it is notable that the rate of water oxidation is far more rapid (minutes compared to hours) for $[(bpy)_2(O)Ru^{V}ORu^{V}(O)(bpy)_2]^{4+}$ compared to $[(bpy)_2(O)Ru^{V}ORu^{III}(py)(bpy)_2]^{4+}$. The key difference between the two may lie in their capabilities as multielectron oxidants. At pH 0, the μ-oxo ions have nearly equivalent reduction potentials (~1.4 V), but for the

mixed-ligand ion, the relevant couple is 1-electron in character (Figure 3)

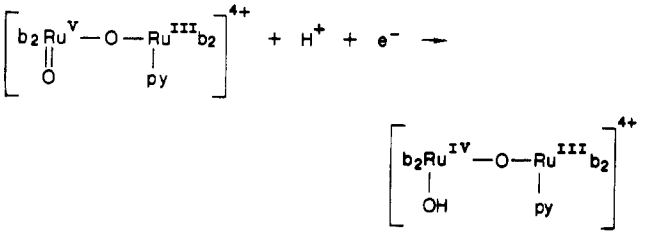

and for the diaqua dimer, it is 3-electron in character[2c]

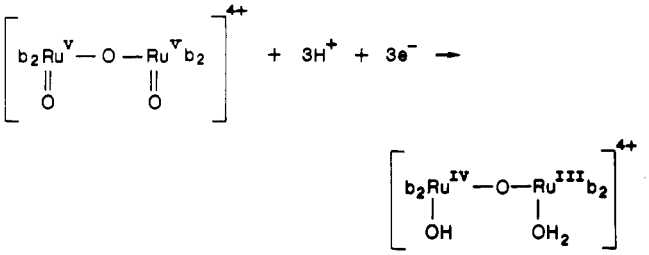

When fully oxidized, the diaqua ion has the thermodynamic capability of direct 4-electron oxidation of H_2O to O_2

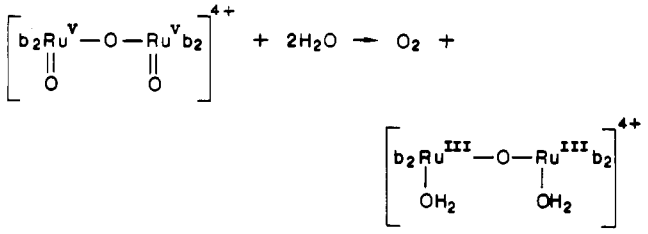

$E^{0'} = 0.28$ V at pH = 1[2c]

The mixed-ligand dimer is also thermodynamically capable of H_2O oxidation but on the basis of a 2-equiv demand

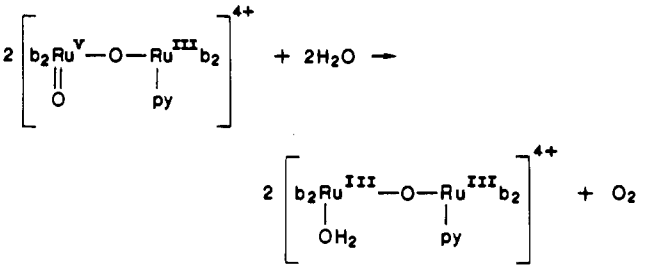

Nonetheless, even the implied ability of the mixed-ligand dimer to oxidize H_2O to O_2 is a significant observation since it suggests that if sufficiently oxidizing, mechanistic pathways may exist which allow a *single* metal site to act as a catalyst for the oxidation of H_2O to O_2.

Acknowledgment. We are grateful to the Centre National de la Recherche Scientific (CNRS), France, to NATO, and to the NIH (Grant GM32296-03) for financial support.

Registry No. $[(bpy)_2(OH_2)RuORu(OH_2)(bpy)_2](ClO_4)_4$, 96364-20-4; $[(bpy)_2(py)RuORu(py)(bpy)_2](ClO_4)_4$, 107985-03-5; $[(bpy)_2(OH_2)RuORu(py)(bpy)_2](ClO_4)_4$, 107985-05-7; $[(bpy)_2(NCMe)RuORu(NCMe)(bpy)_2]^{5+}$, 107985-06-8; $[(bpy)_2(NCMe)RuORu(NCMe)(bpy)_2]^{4+}$, 107985-07-9; $[(bpy)_2(NCMe)RuORu(NCMe)(bpy)_2]^{3+}$, 107985-08-0; $[(bpy)_2(py)RuORu(NCMe)(bpy)_2]^{5+}$, 107985-09-1; $[(bpy)_2(py)RuORu(NCMe)(bpy)_2]^{4+}$, 107985-10-4; $[(bpy)_2(py)RuORu(NCMe)(bpy)_2]^{3+}$, 107985-11-5; $[(bpy)_2(py)RuORu(NCMe)(bpy)_2]^{2+}$, 107985-12-6; $[(bpy)_2(py)RuORu(py)(bpy)_2]^{5+}$, 107985-13-7; $[(bpy)_2(py)RuORu(py)(bpy)_2]^{3+}$, 107985-14-8; $[(bpy)_2(py)RuORu(py)(bpy)_2]^{2+}$, 107985-15-9; $[(bpy)_2(OH_2)RuORu(py)(bpy)_2]^{5+}$, 107985-16-0; $[(bpy)_2(OH_2)RuORu(py)(bpy)_2]^{6+}$, 107985-17-1; $[(bpy)_2(OH)RuORu(py)(bpy)_2]^{3+}$, 107985-18-2; $[(bpy)_2(OH)RuORu(py)(bpy)_2]^{4+}$, 107985-19-3; $[(bpy)_2(py)Ru(H_2O)]^{2+}$, 70702-30-6; $[(bpy)_2(py)Ru(H_2O)]^{3+}$, 75495-08-8; Cl, 16887-00-6; H_2O, 7732-18-5.

Contribution from the Departments of Chemistry, University of Surrey, Guildford, Surrey GU2 5XH, England, and The Open University, Milton Keynes MK7 6AA, England

Ligand Field Effects in the Nuclear Magnetic Shielding of Nitrogen-15 and Cobalt-59 in Bent Nitrosyl Complexes of Cobalt(III)

Paul A. Duffin,[1] Leslie F. Larkworthy,*[1] Joan Mason,*[2] Alan N. Stephens,[1] and Russell M. Thompson[1]

Received August 29, 1986

A range of square-pyramidal complexes of cobalt(III) with a bent apical nitrosyl ligand has been prepared and examined by ^{15}N and ^{59}Co NMR spectroscopy, in a study of nephelauxetic and spectrochemical effects at the metal and nitrogen nuclei in the bent Co–NO chromophore. The basal ligands in this comparison include dithiocarbamate, quadridentate Schiff base or porphine, and bis-chelating diamine or oximate, so as to give S_4, S_2N_2, N_4, OONN, or ONON coordination in the plane and a range of substituents in the chelate and phenylene rings. The shielding of both cobalt and nitrogen tends to decrease with decrease in the M(d) → π*(NO) back-bonding, as indicated by the MN and NO bond distances, the MNO angle and the NO stretching frequency. The shieldings decrease from sulfur to nitrogen to oxygen coligators and also with electron withdrawal by ring substituents (and vice versa), i.e. with decrease in the ligand field splitting and in the nephelauxetism of the coligands. These parallelisms of the cobalt and nitrogen shielding accord with the orbital theory that was developed to explain the bending of the MNO ligand and influences of the metal and coligands. Significant interdependence of spectrochemical and nephelauxetic effects at cobalt and nitrogen arises from the degree of overlap and similarity in energies of the frontier orbitals for the paramagnetic circulation at nitrogen [n(N) → π*(NO)] and at cobalt (d–d).

Introduction

^{15}N NMR spectroscopy is a sensitive indicator of the nature of the nitrosyl ligand, whether linear,[3,4] strongly bent with MNO angle 120–130°,[5–8] partially bent (as e.g. in dinitrosyls),[9] or bridging.[10] In terminal nitrosyls the nitrogen shielding decreases

(1) University of Surrey.
(2) The Open University.
(3) Botto, R. E.; Kolthammer, B. W. S.; Legzdins, P.; Roberts, J. D. *Inorg. Chem.* **1979**, *18*, 2049.
(4) Butler, A. R.; Glidewell, C.; Hyde, A. R.; McGinnis, J. *Inorg. Chem.* **1985**, *24*, 2931.
(5) Bell, L. K.; Larkworthy, L. F.; Mason, J.; Mingos, D. M. P.; Povey, D. C.; Sandell, B. *J. Chem. Soc., Chem. Commun.* **1983**, 125.
(6) Bell, L. K.; Mason, J.; Mingos, D. M. P.; Tew, D. G. *Inorg. Chem.* **1983**, *22*, 3497.

0020-1669/87/1326-2034$01.50/0